PLOS ONE

RESEARCH ARTICLE

Magnetic Clustering Effect during the Association of Biofunctionalized Magnetic Nanoparticles with Biomarkers

Kuen-Lin Chen[1]*, Jean-Hong Chen[2], Su-Hsien Liao[3], Jen-Je Chieh[3], Herng-Er Horng[3], Li-Min Wang[4], Hong-Chang Yang[5]

1 Department of Physics, National Chung Hsing University, Taichung, Taiwan, **2** Department of Materials Engineering, Kun Shan University, Tainan, Taiwan, **3** Institute of Electro-Optical Science and Technology, National Taiwan Normal University, Taipei, Taiwan, **4** Graduate Institute of Applied Physics and Department of Physics, National Taiwan University, Taipei, Taiwan, **5** Department of Electro-optical Engineering, Kun Shan University, Tainan, Taiwan

* klchen@phys.nchu.edu.tw

Citation: Chen K-L, Chen J-H, Liao S-H, Chieh J-J, Horng H-E, Wang L-M, et al. (2015) Magnetic Clustering Effect during the Association of Biofunctionalized Magnetic Nanoparticles with Biomarkers. PLoS ONE 10(8): e0135290. doi:10.1371/journal.pone.0135290

Editor: Vipul Bansal, RMIT University, AUSTRALIA

Received: February 11, 2015

Accepted: July 20, 2015

Published: August 13, 2015

Data Availability Statement: All relevant data are within the paper.

Funding: This work was supported by Ministry of Science and Technology of Taiwan under grants: MOST103-2112-M-005-005-MY3, NSC101-2120-M-168-001 and NSC99-2112-M-168-001-MY3. http://www.most.gov.tw/. The funder had no role in study design, data collection and analysis, decision to publish, or preparation of the manuscript.

Competing Interests: The authors have declared that no competing interests exist.

Abstract

We report herein an investigation into dynamic magnetic clustering that occurs during immunoassays as biofunctionalized magnetic nanoparticles (BMNs) become associated with biotargets. We measure the dynamic effective relaxation time $\tau_{eff}(t)$ and use scanning electron microscopy (SEM) and transmission electron microscopy (TEM) to investigate the C-reactive protein (CRP) as it associates with the BMN Fe_3O_4-antiCRP to form the magnetic cluster Fe_3O_4-antiCRP-CRP. The results indicate that $\tau_{eff}(t)$ increases with increasing association time. In addition, the ration $\Delta\tau_{eff}/\tau_0$ as a function of CRP concentration follows a characteristic logistic function, which provides a basis for estimating the quantity of biomolecules with a detection sensitivity close to 0.1 ppm. After the association, SEM and TEM images show that CRP and Fe_3O_4-antiCRP conjugate to form Fe_3O_4-antiCRP-CRP clusters hundreds of nanometers in size. The SEM and TEM images provide direct evidence of the formation of magnetic clustering.

Introduction

Magnetic detection using biofunctionalized magnetic nanoparticles (BMNs) has recently received considerable attention [1]. In general, biological samples have negligible magnetic backgrounds, therefore a high detection sensitivity and specificity is possible with magnetic detection. Magnetic detection for assaying biomolecules can be done by measuring the magnetic relaxation [2,3], magnetic remanence [4], immunomagnetic reduction (IMR) [5], saturated magnetization [6], reduction in spin-spin relaxation time [7], etc. In immunomagnetic assays, the relaxation in the presence of magnetic clustering during association plays an important role in the detection of biomolecules [1–3,5,7]. Because relaxation mechanism dominates the magnetic variance of sample, it is also the key point of sensitivity limit of the immunomagnetic assay. However, the effects of dynamic magnetic clustering on the characteristics of

relaxation are seldom studied. A previous report [8] discusses the molecule-assisted nanoparticle clustering effect in immunomagnetic reduction (IMR) assay. In that study, clustering effects were manipulated by controlling the concentrations of anti-body-functionalized magnetic nanoparticles in the reagent. Mixed-frequency IMR was used to study the clustering effect, and the experimental results show that particle clustering is enhanced by increasing the concentration of BMNs. In addition, this report claims that the effects of magnetic clustering dominate the increased rate of the IMR signal in mixed-frequency ac susceptibility. It clearly showed that the variance of ac susceptibility due to magnetic clustering effect is a promising method for biomolecule detection. Another report [9] shows real-time Brownian relaxation of BMNs by using a mixed frequency method. Due to clustering effects, the phase delay $\theta(t)$ between magnetization $M(t)$ and applied field $H(t)$ was varied during association. The dynamic behavior of the phase delay angle was studied for assay biomolecules. However, there are few reports on the direct observation of magnetic clustering. Liao et al. [10] reported the time-dependent phase lag of BMNs conjugated with biotargets, as studied with ac magnetic susceptometry for liquid phase immunoassays. Because of the clustering effect, Brownian relaxation of BMNs is suppressed, which in turn enhances the effective relaxation time. By monitoring the dynamic phase lag, a sensitive platform for assaying human C-reactive protein (CRP) was demonstrated. The research goal of the present work is to study the effects of magnetic clustering on the dynamic effective relaxation time $\tau_{eff}(t)$ and provide evidence of magnetic clustering by imaging with scanning electron microscopy (SEM) and transmission electron microscopy (TEM).

In the present work, we report how dynamic magnetic clustering affects $\tau_{eff}(t)$ by measuring the time-dependent phase lag $\theta(t)$ between the applied field $H(t)$ and magnetization $M(t)$ and by imaging with SEM and TEM. The measured phase lag θ is used to estimate τ_{eff} by using the relation $\tan\theta(t) = \omega\tau_{eff}(t)$, where $\theta(t)$ is the time-dependent phase lag of $M(t)$ with respect to $H(t)$, and ω is the angular frequency of the excitation. The BMNs used in this study were anti-goat C-reactive protein coated onto dextran-coated magnetic nanoparticles (Fe_3O_4-antiCRP), and the biotargets were human C-reactive protein (CRP). The results show that τ_{eff} for the reagents increases as association evolves, which we attribute to suppressed Brownian motion due to the presence of magnetic clusters during the association of CRP with Fe_3O_4-antiCRP. We also find that the ratio $\Delta\tau_{eff}/\tau_0$, as a function of CRP concentration follows a universal characteristic logistic function, where $\Delta\tau_{eff} = [\tau_{eff}(t = 0) - \tau_{eff}(t = \infty)]$. Finally, direct evidence of magnetic clustering is provided by SEM and TEM images, which show that the average particle size is about 67.5 ± 11.5 nm for Fe_3O_4-antiCRP, whereas the conjugated clusters of Fe_3O_4-antiCRP-CRP are about 250 nm in size.

Materials and Methods

Materials

The magnetic reagents used in this study were composed of biocompatible magnetic Fe_3O_4 nanoparticles with dextran shell (MagQu Co, Ltd). To synthesize BMNs, polyclonal goat anti-CRP (Sigma-Aldrich, St Louis, MO, USA) was covalently bound to the dextran shell of Fe_3O_4 via −CH = N− [11, 12]. BMN, which consisted of Fe_3O_4-antiCRP, was then dispersed in phosphate buffered saline (PBS) solution with a pH of 7.4. In this study, the mean hydrodynamic diameter of Fe_3O_4 nanoparticle was 45.8 nm with a standard deviation of ±15.0 nm, as determined by dynamic light scattering (Nanotrac-150, Microtrac). Fig 1a shows the magnetization data of the BMN reagent, which was measured by vibrating sample magnetometer (Model 4500, EG&G), and the saturated magnetization was about 0.29 emu/g.

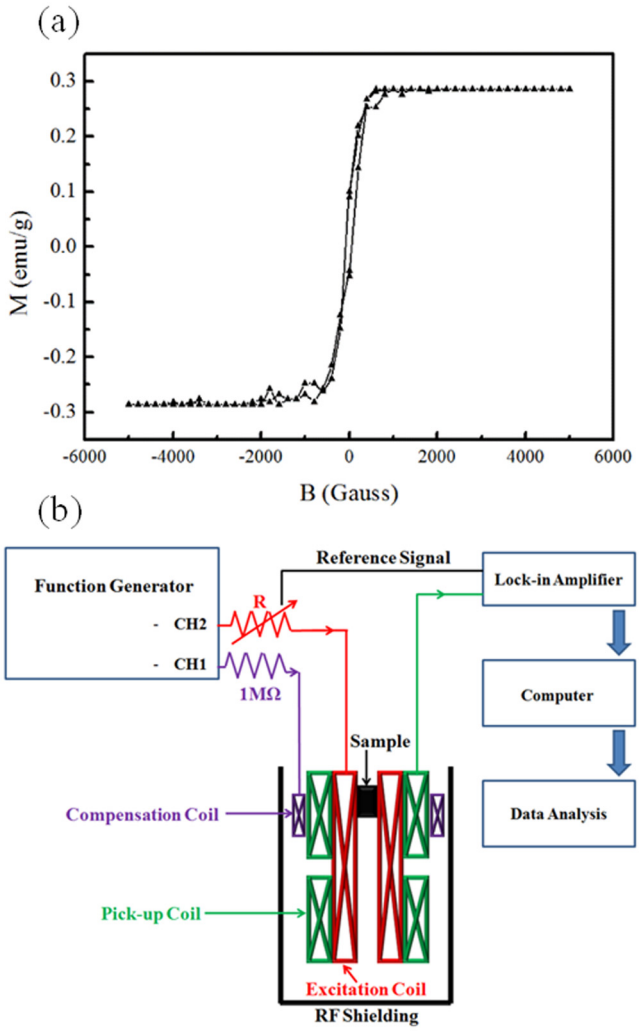

Fig 1. Detection scheme for homemade ac magnetic susceptometer for measuring dynamic $\tau_{eff}(t)$.

doi:10.1371/journal.pone.0135290.g001

Magnetic ac susceptibility measurement

Fig 1b shows the design of the highly balanced homemade ac magnetic susceptometer used to study the time-dependent phase lag angle $\theta(t)$. A detailed description of the measurement technique for characterizing $\theta(t)$ is given in Ref. [10], so we only briefly describe the method here. The sensing unit of the ac susceptometer consists of an input coil, a first-order gradient pick-up coil, and a compensation coil. The first-order gradient pick-up coil is composed of two identical coils wound in opposite directions. The compensation coil is used to precisely balance the sensing unit in the ac susceptometer. Therefore, their phase difference can be adjusted to optimize the balance of the sensing unit. The balance of the sensing coil is defined as the output signal of the two coils of the pick-up coil divided by the output signal from one of the two coils under the excitation of the input coil. This sensing unit achieves a balance of 30 parts per trillion (ppt). The signal from the pick-up coil and the reference frequency component from the function generator were input to a lock-in amplifier, and the time-dependent $\tau_{eff}(t)$ was estimated by using $\tan\theta(t) = \omega\tau_{eff}(t)$.

SEM and TEM images

The morphologies of Fe_3O_4, Fe_3O_4-antiCRP nanoparticles, and CRP conjugated Fe_3O_4-antiCRP were investigated with field-emission scanning electron microscope (FESEM) (Hitachi S-4700), and field emission gun transmission electron microscope (FEI-TEM) (Philips Tecnai F20 G2). Before taking the electron microscopy, the nanoparticles and magnetic clusters were dispersed in a super-diluted solvent (1:50) and then drying the magnetic samples under vacuum at room temperature for 48 hours.

Results and Discussion

By means of the surface modification for specific biotargets, BMN is a good reagent for the immunomagnetic assay. By means of antigen-antibody interaction, BMNs will be gathered to form bigger clusters when the BMN reagent is mixed with antigen. Therefore, the magnetic characteristics of BMN reagent are going to change, and the variation of magnetic characteristics could be used to identify the quantity of antigen. An illustration depicting the human CRP, Fe_3O_4-antiCRP, and magnetic clusters consisting of Fe_3O_4-antiCRP-CRP is shown in Fig 2. In this work, we used magnetic ac susceptibility measurement to investigate the clustering effect of antiCRP coated BMNs interacting with CRP antigen. To study the phase lag dynamics $\theta(t)$, 60 μl of Fe_3O_4-antiCRP reagent of which saturated magnetization is 0.29 emu/g was mixed with 40 μl of CRP with concentrations varying from 0.1 to 10 ppm (1 ppm = 1 μg/mL). $\theta(t)$ is also related to $\tau_{eff}(t)$ by $\tan\theta(t) = \omega\tau_{eff}(t)$, where $f = \omega/(2\pi) = 9$ kHz is the excitation frequency used in the experiment. The presence of dynamic magnetic clustering during the association affects $\theta(t)$, which in turn modifies $\tau_{eff}(t)$. We investigated the dynamics of $\theta(t)$ and $\tau_{eff}(t)$ via lock-in detection, as shown in Fig 1b. The results show that τ_{eff} increases and saturates when association is complete. Furthermore, the ratio $\Delta\tau_{eff}/\tau_0$ as a function of CRP concentration provides a basis for estimating the quantity of biomolecules. Finally, we directly observed the formation of magnetic clusters by SEM and TEM images.

Fig 3a shows the time-dependent $\tau_{eff}(t)$ after mixing the reagent (0.29 emu/g) of Fe_3O_4-antiCRP with 5 ppm CRP at 300 K. The results show that τ_{eff} increases from $\tau_{eff} = 0.62$ μs at t = 0 to $\tau_{eff} = 0.83$ μs at t = 4800 s. Fig 3b shows τ_{eff} as a function of time after mixing Fe_3O_4-antiCRP with 0.1 ppm CRP at 300 K. The results show that τ_{eff} increases from 0.62 μs at t = 0

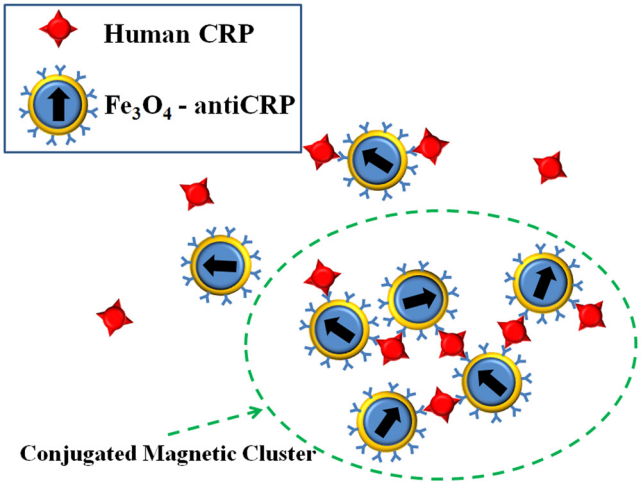

Fig 2. Illustration depicting conjugation of human CRP and Fe_3O_4-antiCRP to form Fe_3O_4-antiCRP-CRP cluster.

doi:10.1371/journal.pone.0135290.g002

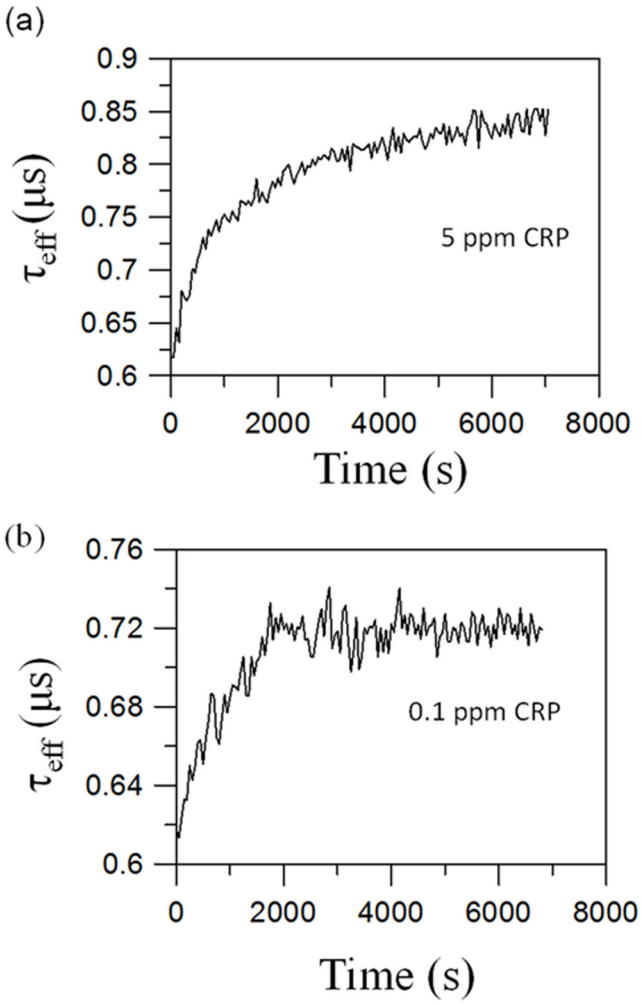

Fig 3. Time-dependent $\tau_{eff}(t)$ for assaying (a) 5.0 ppm and (b) 0.1 ppm of human CRP. Upon conjugating Fe_3O_4-antiCRP and CRP antigen, $\tau_{eff}(t)$ becomes larger and gradually approaches equilibrium.

doi:10.1371/journal.pone.0135290.g003

to τ_{eff} = 0.72 μs at t = 1800 s. The increase of τ_{eff} is attributed to the formation of magnetic clusters during the association, which depresses the Brownian relaxation. Completing the association of 5 ppm CRP with the reagents takes 1.5 hours. The association time decreases to 0.5 hours to assay 0.1 ppm CRP. Consequently, a shorter association time results from reducing the CRP concentration. Thus, characterizing the dynamics of τ_{eff} is done with a detection sensitivity of 0.1 ppm.

The mechanism behind the dynamics of τ_{eff} for BMNs during association can be understood as follows: Consider the ac magnetic susceptibility of BMNs, $\chi(\omega)$, in an applied ac magnetic field. $\chi_{ac}(\omega,t)$ is a function of τ_{eff} and has angular frequency ω. The magnetic susceptibility $\chi_{ac}(\omega,t)$ can be expressed as [13,14]

$$\chi_{ac}(\omega,t) = \chi' + i\chi'' \tag{1}$$

$$= \chi_0 \left\{ \left[\frac{1}{1+(\omega\tau_{eff})^2} \right]^2 + \left[\frac{(\omega\tau_{eff})}{1+(\omega\tau_{eff})^2} \right]^2 \right\}^{1/2} e^{-i\theta(t)}, \tag{2}$$

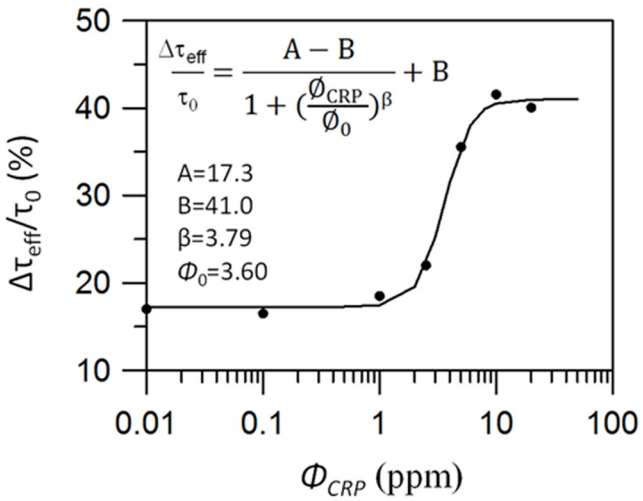

Fig 4. $\Delta\tau_{eff}/\tau_0$ as a function of CRP concentration in semilog plot at 300 K. τ_0 is the effective relaxation time at t = 0. $\Delta\tau_{eff}$ is the effective relaxation time between the beginning and the end of the reaction, and is defined as $\Delta\tau_{eff} = [\tau_{eff}\ (t = 0) - \tau_{eff}\ (t = 6000\ s)]$.

doi:10.1371/journal.pone.0135290.g004

where χ_0 is the component of χ_{ac} at $\omega = 0$, $i = (-1)^{1/2}$, $\chi' = \chi_0\{1/[1+(\omega\tau_{eff})^2]\}$, $\chi'' = \chi_0\{(\omega\tau_{eff})/[1+(\omega\tau_{eff})^2]\}$, and θ is the phase lag. $\chi''(t)/\chi'(t) = \tan\theta$, so Eqs 1 and 2 lead to $\tan\theta = \omega\tau_{eff}$. For BMNs, τ_{eff} can be written as

$$1/\tau_{eff} = \sum_i 1/\tau_{i,B} + \sum_i 1/\tau_{i,N} = 1/\tau_B + 1/\tau_N, \quad (3)$$

where Σ_i indicates summation over all BMN sizes, $1/\tau_{i,B}$ is the relaxation rate due to the Brownian motion of nanoparticle i, and $1/\tau_{i,N}$ is the relaxation rate due to the Néel relaxation of nanoparticle i. Using $\tan\theta(t) = \omega\tau_{eff}(t)$, the dynamics of τ_{eff} can be understood by monitoring the time evolution of θ. As Fe_3O_4-antiCRP conjugates with CRP, magnetic clusters form, which depresses the Brownian motion and in turn increases τ_{eff}.

Fig 4 shows the ratio $\Delta\tau_{eff}/\tau_0$ as a function of CRP concentration at 300 K, expressed on a semilog plot, where $\Delta\tau_{eff} = [\tau_{eff}\ (t = 0) - \tau_{eff}\ (t = 6000\ s)]$ when the association of CRP with Fe_3O_4-antiCRP is complete. The effective relaxation time $\tau_0 = 0.62$ μs at t = 0 is derived from $\tan\theta = \omega\tau_{eff}$. When the concentration of CRP is 20 ppm, $\Delta\tau_{eff} = 0.26$ μs ($\Delta\tau_{eff}/\tau_0 = 41.9\%$) and, when the CRP concentration decreases to 0.1 ppm, $\Delta\tau_{eff}$ saturates at 0.11 μs ($\Delta\tau_{eff}/\tau_0 = 17.7\%$). If we further reduce the CRP concentration to 0.01 ppm, $\Delta\tau_{eff}$ remains at ~0.11 μs, which is close to the experimental noise. Thus, for the present system, the lowest concentration for which detection is possible is 0.1 ppm.

The ratio $\Delta\tau_{eff}/\tau_0$ as a function of CRP concentration follows a characteristic logistic function [15] given by

$$\Delta\tau_{eff}/\tau_0 = \frac{A-B}{1+\left(\frac{\phi_{CRP}}{\phi_0}\right)^{\beta}} + B \quad (4)$$

where A and B are dimensionless parameters, and ϕ_{CRP} and ϕ_0 are in the units of ppm (or μg/mL). The solid line in Fig 4 shows a fit with parameters $A = 17.3$, $B = 41.0$, $\beta = 3.79$, and $\phi_0 = 3.60$ ppm. Because of environmental and system noise, $\Delta\tau_{eff}/\tau_0$ is nonzero at $\phi_{CRP} = 0$. In practical applications, this universal logistic function provides a basis for estimating the quantity of biomolecules [16].

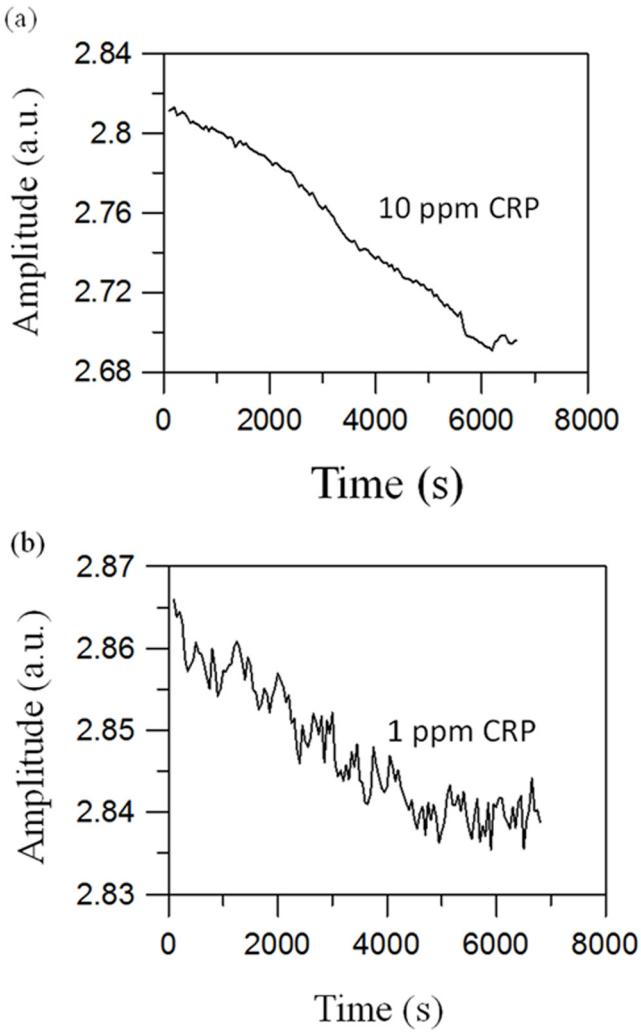

Fig 5. Representative amplitude of ac susceptibility as a function of time when assaying (a) 10 ppm CRP and (b) 1.0 ppm CRP. The increase in τ_{eff} induces a reduction of χ_{amp} during particle association.

doi:10.1371/journal.pone.0135290.g005

From Eq 2 we obtain the magnitude of the ac susceptibility, χ_{amp}, which is given by

$$\chi_{amp}(t) = \frac{\chi_0}{[1 + (\omega\tau_{eff}(t))^2]^{1/2}}. \quad (5)$$

Based on Eq 5 we see that an increase in τ_{eff} induces a reduction of χ_{amp} after association. Additionally, assaying a higher concentration of CRP leads to a larger reduction in $\Delta\chi$, which is observed in experiments. Fig 5 shows the time-dependent amplitude of the ac susceptibility for assaying 10 and 1.0 ppm CRP. The susceptibility $\chi(t)$ decreases from 2.83 μV at t = 0 to 2.70 μV at t = 6000 s when assaying 10 ppm CRP, and from 2.87 μV at t = 0 to 2.84 μV at t = 6000 s when assaying 1 ppm CRP. The percent reduction $\Delta\chi/\chi_0 \times 100\% = 4.6\%$ when assaying 10 ppm CRP, and $\Delta\chi/\chi_0$ was reduced to 0.8% when assaying 1.0 ppm CRP.

Although the measurement of ac susceptibility provides evidence for magnetic clustering from the conjugation of CRP and Fe_3O_4-antiCRP, the aggregation is not directly observed.

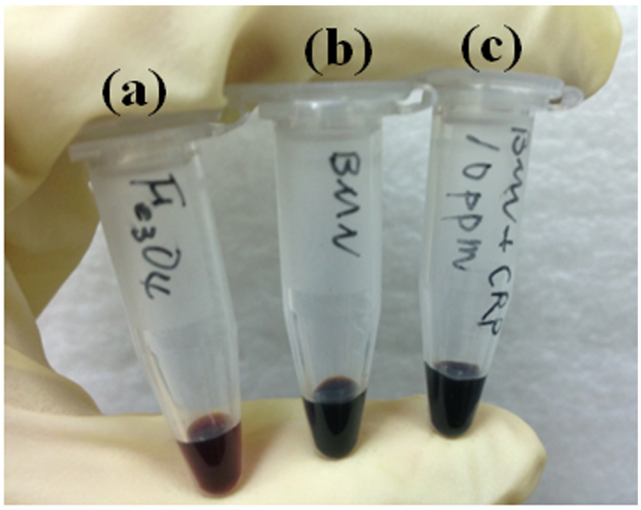

Fig 6. The picture of the solutions of Fe_3O_4 nanoparticles, Fe_3O_4-antiCRP, and CRP conjugated Fe_3O_4-antiCRP after 1.5 hours mixture. (a) Fe_3O_4 60μl + PBS 40μl, (b) Fe_3O_4-antiCRP 60μl + PBS 40μl, and (c) Fe_3O_4-antiCRP 60μl + 10 ppm CRP antigen 40μl after 1.5 hours.

doi:10.1371/journal.pone.0135290.g006

Fig 6 is the picture of the solutions of Fe_3O_4 nanoparticles, Fe_3O_4-antiCRP, and CRP conjugated Fe_3O_4-antiCRP after 1.5 hours mixture. It clearly shows that there are not any observable aggregations and precipitations in these solutions even though CRP had conjugated with Fe_3O_4-antiCRP for 1.5 hours. Therefore, we used the SEM and TEM to investigate the effect of clustering. The inhomogeneity of BMNs usually leads to large variations in results. Thus, to enhance the stability and reproducibility of assaying biomarkers, highly homogeneous Fe_3O_4 is necessary for the Fe_3O_4-antiCRP preparation. We used SEM to check the homogeneity of the Fe_3O_4 use for BMN synthesis. Fig 7a shows a typical SEM image of Fe_3O_4, and Fig 7b shows a magnified SEM image of Fe_3O_4, with the particle size indicated. The diameters of the Fe_3O_4 are almost all the same, which indicates that the Fe_3O_4 used in the BMN synthesis is highly homogeneous. The particle size of Fe_3O_4 was measured to be ~ 48.4 ± 9.9 nm on average, which is very close to the result obtained with dynamic light scattering.

Fig 8a shows a TEM image of the reagent composed of Fe_3O_4-antiCRP. The average particle size varies from (60 ± 5.0) to (70 ± 5.0) nm with an average size of ~ 67.5 ± 11.5 nm. The core of Fe_3O_4 and the outer shell of the coated antiCRP are apparent. Moreover, Fig 8b shows a TEM image of CRP. The average particle size of CRP is 10 ± 0.5 nm which is consistent with the data reported in Ref. [17]. TEM shows that CRP conjugates with Fe_3O_4-antiCRP upon adding CRP to the reagent of Fe_3O_4-antiCRP. Fig 8c shows a TEM image of the magnetic cluster of Fe_3O_4-antiCRP-CRP at t = 1 h after mixing CRP with Fe_3O_4-antiCRP. In addition to the unconjugated CRPs, the conjugated Fe_3O_4-antiCRP-CRP single particles and the Fe_3O_4-antiCRP-CRP cluster are also apparent. These results show clearly that CRP adheres to the surface of Fe_3O_4-antiCRP via antigen-antibody interactions [18] and aggregates Fe_3O_4-antiCRP together to form bigger clusters. The size of magnetic clusters of Fe_3O_4-antiCRP-CRP varies from ~ 80 to 250 nm at t = 1 h and increases with association time. Thus, the effect of magnetic clustering is directly revealed by SEM and TEM.

A method to conduct a wash-free magnetically labeled immunoassay using mixed excitation frequencies was previously proposed [4]. As a detection method, two excitation currents at frequencies of f_1 and f_2 were applied to the excitation coils. The reduction of χ_{ac} for BMNs conjugated with biotargets was analyzed at the target frequency f_1+2f_2 to qualitatively determine the

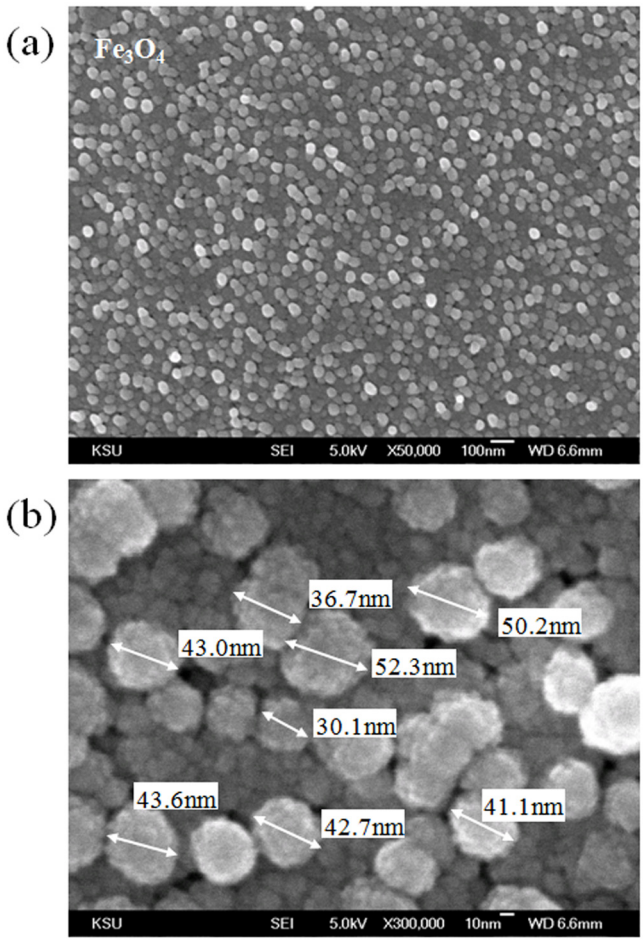

Fig 7. SEM images of (a) Fe_3O_4 applied to BMN synthesis. (b) Magnified SEM picture of Fe_3O_4 with the particle size indicated. The average size of Fe_3O_4 particles is ~ 48.4 ± 9.9 nm.

doi:10.1371/journal.pone.0135290.g007

amount of biotarget, where f_1 and f_2 are the excitation frequencies of the input coils. The IMR assay in the frequency domain was used to assay CRP [19,20]. Real-time Brownian relaxation of BMNs was also investigated by using a mixed frequency method, and the phase delay between $M(t)$ and $H(t)$ was investigated to detect biomolecules [9]. In the present work, the phase delay of M with respect to H and the reduction of χ_{amp} was investigated to assay CRP by using single frequency ac susceptometry. The results indicate that τ_{eff} increases with association time. We attribute this result to the suppression of Brownian motion, which is due to the magnetic clustering during association. Additionally, the ratio $\Delta\tau_{eff}/\tau_0$ follows a logistic function, which provides a basis for estimating the quantity of biomolecules. Furthermore, the effect of magnetic clustering is directly revealed via SEM and TEM.

CRP levels in blood are key indicators of infectious disease, noninfectious disease, and acute tissue. The normal concentration in healthy human serum is usually less than 10 μg/mL, which slightly increases with age. Higher levels are found in late-pregnancy women and in people with mild inflammation or viral infection (10–40 μg/mL), in people with active inflammation or bacterial infection (40–200 μg/mL), and in people with severe bacterial infections or burns (>200 μg/mL) [21]. By using BMNs and the technique of mixed-frequency ac susceptmetry, quantitative immunoassays for CRP were demonstrated in clinical diagnoses [22]. In the

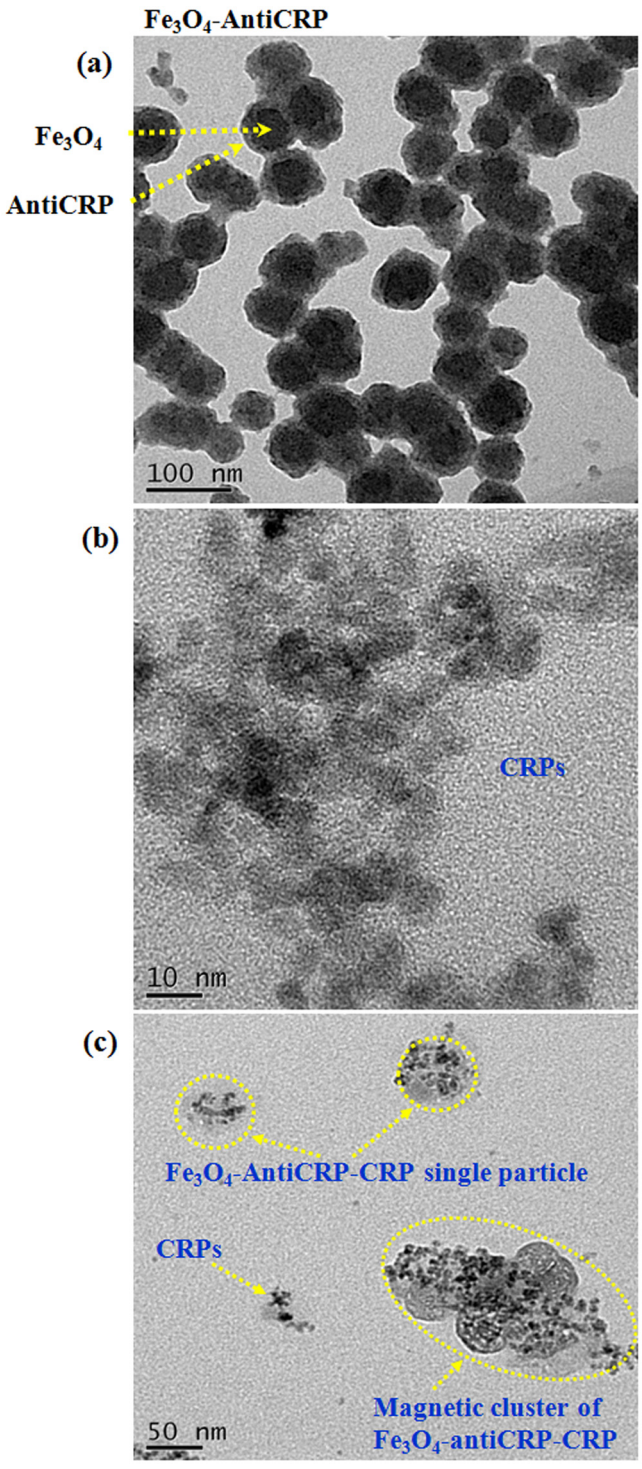

Fig 8. TEM images of (a) Fe_3O_4-antiCRP nanoparticles and (b) CRP antigens. (c) TEM image of conjugated Fe_3O_4-antiCRP-CRP particles and cluster after association time of 1 h.

doi:10.1371/journal.pone.0135290.g008

present work, we investigate the dynamics of τ_{eff} and use SEM and TEM to show magnetic clustering. By using $\theta(t)$ and $\tau_{eff}(t)$, this method provides a detection sensitivity of 0.1 ppm.

Conclusions

We investigate the dynamics of $\tau_{eff}(t)$ during association of Fe_3O_4-antiCRP with CRP. The results show that τ_{eff} increases and saturates when association is complete. In addition, the ratio $\Delta\tau_{eff}/\tau_0$ as a function of CRP concentration follows a characteristic logistic function, which provides a basis for estimating the quantity of biomolecules and a detection sensitivity of 0.1 ppm is demonstrated. Finally, SEM and TEM images directly revealed the formation of magnetic clusters. This magnetic detection platform is promising for future use in assaying a broad number of biomarkers, such as viruses, proteins, tumors, etc.

Author Contributions

Conceived and designed the experiments: KLC SHL HCY. Performed the experiments: KLC JHC SHL. Analyzed the data: KLC JHC SHL. Contributed reagents/materials/analysis tools: JHC JJC HEH LMW HCY. Wrote the paper: KLC HCY.

References

1. Tamanaha CR, Mulvaney SP, Rife JC, Whitman LJ (2008) Magnetic labeling, detection, and system integration. Biosens Bioelectron 24: 1–13. doi: 10.1016/j.bios.2008.02.009 PMID: 18374556
2. Kötitz R, Weitschies W, Trahms L, Brewer W, Semmler W (1999) Determination of the binding reaction between avidin and biotin by relaxation measurements of magnetic nanoparticles. J Magn Magn Mater 194: 62–68.
3. Lee SK, Myers WR, Grossman HL, Cho H-M, Chemla YR, Clarke J (2002) Magnetic gradiometer based on a high-transition temperature superconducting quantum interference device for improved sensitivity of a biosensor. Appl Phys Lett 81: 3094.
4. Enpuku K, Minotani T, Gima T, Kuroki Y, Itoh Y, Yamashita M, et al. (1999) Detection of Magnetic Nanoparticles with Superconducting Quantum Interference Device (SQUID) Magnetometer and Application to Immunoassays. Jpn J Appl Phys 38: L1102–L1105.
5. Hong CY, Wu CC, Chiu YC, Yang SY, Horng HE, Yang HC (2006) Magnetic susceptibility reduction method for magnetically labeled immunoassay. Appl Phys Lett 88: 212512.
6. Horng HE, Yang SY, Hong CY, Liu CM, Tsai PS, Yang HC, et al. (2006) Biofunctionalized magnetic nanoparticles for high-sensitivity immunomagnetic detection of human C-reactive protein. Appl Phys Lett 88: 252506.
7. Lee H, Sun E, Ham D, Weissleder R (2008) Chip–NMR biosensor for detection and molecular analysis of cells. Nat Med 14: 869–874. doi: 10.1038/nm.1711 PMID: 18607350
8. Yang SY, Chieh JJ, Huang KW, Yang CC, Chen TC, Ho CS, et al. (2013) Molecule-assisted nanoparticle clustering effect in immunomagnetic reduction assay. J Appl Phys 113: 144903.
9. Tu L, Jing Y, Li Y, Wang JP (2011) Real-time measurement of Brownian relaxation of magnetic nanoparticles by a mixing-frequency method. Appl Phys Lett 98: 213702.
10. Liao SH, Yang HC, Horng HE, Chieh JJ, Chen KL, Chen HH, et al. (2013) Time-dependent phase lag of biofunctionalized magnetic nanoparticles conjugated with biotargets studied with alternating current magnetic susceptometor for liquid phase immunoassays. Appl Phys Lett 103: 243703.
11. Jiang W, Yang HC, Yang SY, Horng HE, Hung JC, Chen YC, et al. (2004) Preparation and properties of superparamagnetic nanoparticles with narrow size distribution and biocompatible. J Magn Magn Mater 283; 210–214.
12. Yang SY, Yang CC, Horng HE, Shih BY, Chieh JJ, Hong CY, et al. (2013) Experimental study on low-detection limit for immunomagnetic reduction assays by manipulating reagent entities. IEEE Trans Nanotechnol 12:65–68.
13. Rosensweig RE (2002) Heating magnetic fluid with alternating magnetic field. J Magn Magn Mater 252: 370–374.
14. Yang CC, Yang SY, Chen HH, Weng WL, Horng HE, Chieh JJ, et al. (2012) Effect of molecule-particle binding on the reduction in the mixed-frequency alternating current magnetic susceptibility of magnetic bio-reagents. J Appl Phys 112: 024704.

15. Frantzen F, Faaren AL, Alfheim I, Nordhei AK (1998) Enzyme conversion immunoassay for determining total homocysteine in plasma or serum. Clin Chem 44: 311–316. PMID: 9474030

16. Yang CC, Yang SY, Chieh JJ, Horng HE, Hong CY, Yang HC (2012) Universal Behavior of Biomolecule-Concentration-Dependent Reduction in AC Magnetic Susceptibility of Bioreagents. IEEE Magn Lett 3: 1500104.

17. Osmand AP, Friedenson B, Gewurz H, Painter RH, Hofmann T, Shelton E (1977) Characterization of C-reactive protein and the complement subcomponent C1t as homologous proteins displaying cyclic pentameric symmetry (pentraxins). Proc Natl Acad Sci USA 74: 739–743. PMID: 265538

18. van Oss CJ, Good RJ, Chaudhury MK (1986) Nature of the antigen-antibody interaction: Primary and secondary bonds: optimal conditions for association and dissociation. J Chromatogr B 376: 111–119.

19. Chieh JJ, Yang SY, Horng HE, Jian ZF, Wang WC, Horng HE, et al. (2008) Hyper-high-sensitivity wash-free magnetoreduction assay on biomolecules using high-T_c superconducting quantum interference devices. J Appl Phys 103: 014703.

20. Hong CY, Chen WS, Jian ZF, Yang SY, Horng HE, Yang LC, et al. (2007) Wash-free immunomagnetic detection for serum through magnetic susceptibility reduction. Appl Phys Lett 90: 074105.

21. Clyne B, Olshaker JS (1999) The C-reactive protein. J Emerg Med 17: 1019–1025. PMID: 10595891

22. Chang CH, Lai ZX, Lin HL, Yang CC, Chen HH, Yang SY, et al. (2012) Use of immunomagnetic reduction for C-reactive protein assay in clinical samples. Intern J Nanomed 7: 4335–4340.